

Federated Fine-Tuning of Foundation Models via Probabilistic Masking

Vasileios Tsouvalas¹, Yuki M Asano², Aaqib Saeed¹

¹Eindhoven University of Technology, ²University of Amsterdam

Abstract

Foundation Models (FMs) have revolutionized machine learning with their adaptability and high performance across tasks; yet, their integration into Federated Learning (FL) is challenging due to substantial communication overhead from their extensive parameterization. Current communication-efficient FL strategies, such as gradient compression, reduce bitrates to around 1 bit-per-parameter (bpp). However, these approaches fail to harness the characteristics of FMs, with their large number of parameters still posing a challenge to communication efficiency, even at these bitrate regimes. In this work, we present *DeLtaMask*, a novel method that efficiently fine-tunes FMs in FL at an ultra-low bitrate, well below 1 bpp. *DeLtaMask* employs stochastic masking to detect highly effective subnetworks within FMs and leverage stochasticity and sparsity in client masks to compress updates into a compact grayscale image using probabilistic filters, deviating from traditional weight training approaches. Our comprehensive evaluations across various datasets and architectures demonstrate *DeLtaMask* efficiently achieves bitrates as low as 0.09 bpp, enhancing communication efficiency while maintaining FMs performance, as measured on 8 datasets and 5 pre-trained models of various network architectures.

1 Introduction

Federated learning (FL) enables collaborative training of neural network models directly on edge devices (referred to as clients), locally with on-device data [Konečný et al. \(2016\)](#). FL comprises multiple federated rounds, which involve server-to-client model updates dispatch, local training by clients, and server-side aggregation (e.g., via FedAvg [McMahan et al. \(2017\)](#)) of clients' model updates, iteratively performed until model convergence. Despite its appealing properties for users' privacy, FL requires constant models' updates transfer between server and clients, which poses a challenge in terms of communication efficiency. This becomes even more critical when the clients are resource-constrained edge devices, which operate under limited transmission bandwidth and strict computational and energy constraints.

Recent advances in FL have led to a variety of methods aimed at enhancing communication efficiency, particularly by reducing the data volume exchanged in each federated round. These strategies often employ gradient compression techniques, including sparsification [Lin et al. \(2020\)](#); [Aji and Heafield \(2017\)](#), quantization [Alistarh et al. \(2017\)](#); [Aji and Heafield \(2017\)](#); [Vargaftik et al. \(2022, 2021\)](#), and low-rank approximation [Mohtashami et al. \(2022\)](#); [Mozaffari et al. \(2022\)](#), which are pivotal in streamlining data transmission. Alongside this research, the "Lottery Ticket Hypothesis" [Frankle and Carbin \(2019\)](#) has paved the way for FL training regimes that diverge from traditional weight updates. Here, the focus has shifted toward identifying and cultivating high-potential subnetworks within randomly initialized neural models [Li et al. \(2021a\)](#); [Vallapuram et al. \(2022\)](#); [Li et al. \(2020\)](#); [Isik et al. \(2023b\)](#). Such subnetworks demonstrate good performance without the need for extensive weight adjustments, offering a new path to minimize FL communication overhead. Notably, techniques like FedMask [Li et al. \(2021a\)](#) and FedPM [Isik et al. \(2023b\)](#), which learn binary masks on top of random dense networks, can effectively reduce bitrate from 32 to 1 bit-per-parameter (bpp). However, jointly learning effective subnetworks in large, randomly initialized models, can extend their training duration and adversely affect model convergence.

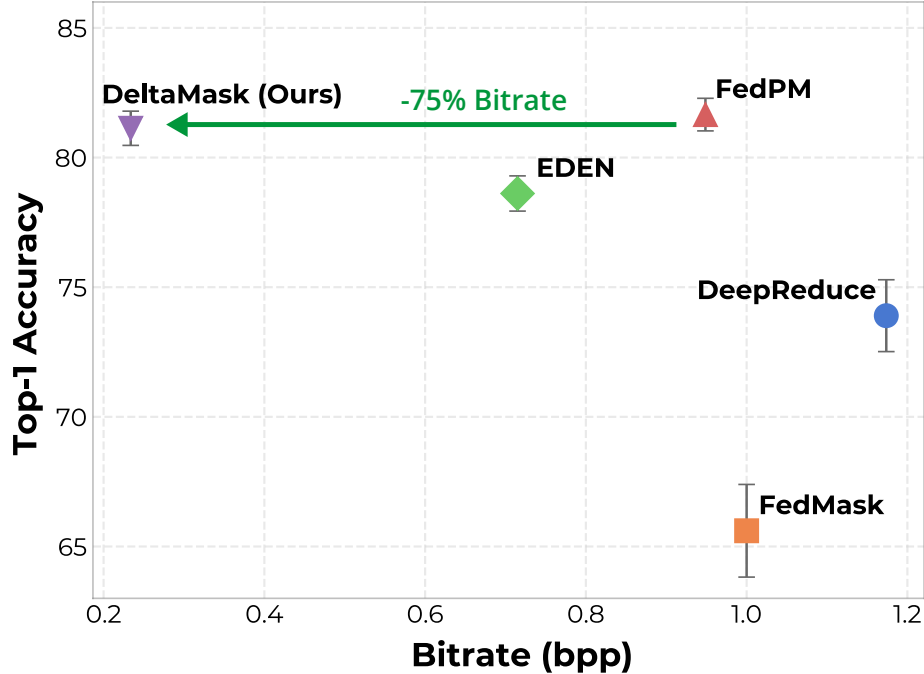


Figure 1: DeltaMask (Ours) vs. state-of-the-art communication-efficient FL techniques when using CLIP pre-trained ViT-B/32, results are averaged over 8 datasets.

Leveraging the advancements in self-supervised learning, Foundation Models (FMs) have brought significant advancement across various machine learning domains with their remarkable representation quality. Models like CLIP [Radford et al. \(2021\)](#) and DINOv2 [Oquab et al. \(2023\)](#) demonstrate rapid adaptability to diverse tasks, achieving unmatched performance in several downstream applications. Notably, recent developments have seen vision FMs, such as the ViT models, expand to billions of parameters [Dehghani et al. \(2023\)](#), exemplifying the scale and complexity of modern FMs. In turn, and as an alternative to traditional fine-tuning, masking strategies have emerged [Mallya et al. \(2018\)](#); [Zhao et al. \(2020\)](#) in a centralized setting, where selective binary masks are learned on top of frozen pre-trained weights, matching the performance of full fine-tuning. Nevertheless, the high parameter count of FMs inhibits their expansion into federated settings due to the substantial communication overhead, even at a bitrate of 1 bpp, thereby limiting their potential to tap into the valuable data available in distributed (decentralized) environments.

To bridge the gap between the high-performance potential of Foundation Models (FMs) and the practical constraints of federated settings, we introduce DeltaMask, an approach designed to fine-tune FMs to various downstream tasks in federated settings with significantly reduced bitrate requirements (see Figure 1). Inspired by the sparse mask updates between subsequent federated rounds, which naturally occur due to the rapid adaptability of FMs, our approach combines stochastic masking with probabilistic filters to find high-performing subnetworks within pre-trained FM, while operating in an ultra-low bitrate regime. This paves the way for fine-tuning FMs in federated settings without the massive communication burden caused by their large number of parameters. Concisely, the main contributions of our work are as follows:

- We present a simple, yet effective, method termed DeltaMask, to allow fine-tuning of FMs in federated settings in a highly communication-efficient manner.
- We combine stochastic binary masks with probabilistic filters to compactly communicate mask updates and reduce bitrate bpp below 0.1.
- Our evaluation across 8 datasets and 5 pre-trained models of various network architectures demonstrate strong effectiveness of DeltaMask to fine-tune FMs compared to existing FL techniques.

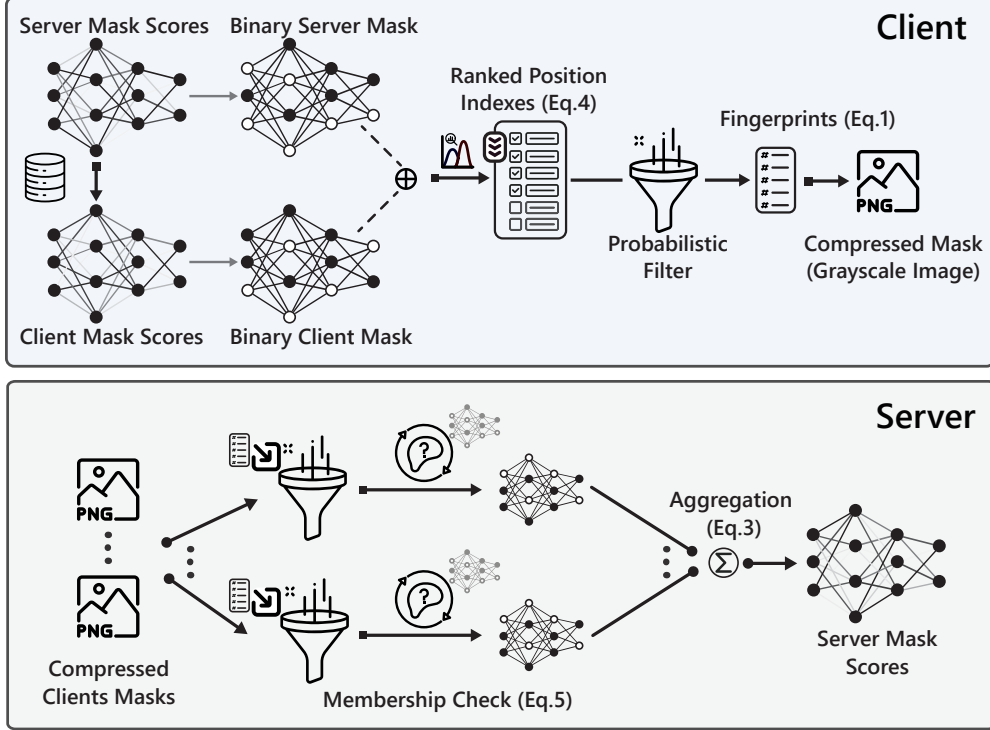


Figure 2: Overview of DeltaMask: Discrepancies between received and learned masks are cataloged and ranked based on the relative entropy between server and client mask probabilities. Only essential updates populate a binary fuse filter through a top_k mechanism, extracting hashed entries compressed into a single grayscale image via lossless processing. Server reconstructs clients’ masks through membership queries across all positions, subsequently updating the global mask with the Bayesian aggregation.

2 Related Work

Communication-Efficient FL. Enhancing communication efficiency in FL can be achieved through fast adaptation to downstream tasks by utilizing methods such as adaptive optimizers [Reddi et al. \(2021\)](#) or efficient client-sampling processes [Chen et al. \(2022\)](#) that accelerate the convergence rate and, consequently, minimize the data transmission requirement. Alternatively, model updates can be compressed using gradient compression strategies like sparsification [Lin et al. \(2020\)](#); [Aji and Heafield \(2017\)](#), quantization [Vargaftik et al. \(2022, 2021\)](#); [Kostopoulou et al. \(2021\)](#), and low-rank approximation [Mohtashami et al. \(2022\)](#); [Mozaffari et al. \(2022\)](#), which reduce the volume of data transmitted during the learning process by shrinking the size of updates communicated in each round. Likewise, training masks over densely initialized networks has been explored to provide communication efficiency between client and server [Isik et al. \(2023b\)](#); [Vallapuram et al. \(2022\)](#). In [Isik et al. \(2023b\)](#), stochastic mask training was utilized to sample binary masks from locally trained mask probabilities using a Bernoulli distribution, which were then transmitted to the server.

To reduce the bitrate below 1 bpp, [Isik et al. \(2023b\)](#) employs arithmetic coding [Rissanen and Langdon \(1979\)](#) to encode masks based on the sparsity level (frequency of activations). However, arithmetic coding is characterized by computational complexity and intricate implementation, while its efficacy is limited due to the stochasticity of mask sampling, which leads to inconsistent mask activations. In contrast, our approach improves stochastic mask training over pre-trained FMs, introducing a novel lightweight communication protocol that employs probabilistic filters by leveraging the sparsity in subsequent mask changes. Alongside [Isik et al. \(2023b\)](#), we align DeltaMask with gradient compression baselines, such as EDEN [Vargaftik et al. \(2022\)](#) and DeepReduce [Kostopoulou et al. \(2021\)](#), which operate in a similar bitrate regime (≈ 1 bpp).

Masking Neural Networks. Masks learned using gradient descent on pre-trained models can yield sub-networks with performance in parallel to conventional fine-tuning for various downstream tasks, as first demonstrated by Mallya et al. (2018). A similar observation was evident in Zhao et al. (2020), where masking was utilized on language models. Following the Lottery Ticket Hypothesis Frankle and Carbin (2019), the same idea was expanded to randomly initialized densely connected networks Zhou et al. (2020); Ramanujan et al. (2020); Aladago and Torresani (2021), where mask training was shown to act as an alternative form of weight training. These concepts were applied in FL in Li et al. (2021a); Vallapuram et al. (2022); Isik et al. (2023b) to deal with different challenges in FL, such as personalization, communication efficiency and privacy. Our masking method is functionally equivalent to that of Isik et al. (2023b), however, we focus on pre-trained foundation models and further reduce the required bitrate below the 1 bpp threshold by communicating the minimal information to reconstruct the clients’ masks through probabilistic filters Graf and Lemire (2022).

3 Methodology

3.1 Preliminaries

Probabilistic Filters. Probabilistic filters are specialized data structures that map a universe of keys, denoted as \mathcal{U} , of varying bit lengths, to fixed-size bit values, thereby compacting real-world data representations effectively. They achieve this by using hash functions to transform and store data in a uniformly distributed array, known as the fingerprints \mathcal{H} . This compact representation \mathcal{H} facilitates efficient membership checking, with an adjustable rate of false positives — where a non-member might be incorrectly identified as a member — while ensuring zero false negatives. There are multiple variations of probabilistic filters, we focus on *binary fuse filters* (BFuse) Graf and Lemire (2022), which are known for their exceptional space efficiency and computational effectiveness. These filters offer a space efficiency of 8.62 bits per entry and a low false positive rate between (up to 2^{-32}).

Formally, an m -wise BFuse utilizes m distinct hash functions $h_j : \{0, 1, \dots, 2^n - 1\} \rightarrow \{1, 2, \dots, s\}$, for $j = 1, \dots, m$, where s denotes the size of the fingerprints array, \mathcal{H} . Let $f : \mathbb{N} \rightarrow \{0, 1, \dots, 2^n - 1\}$ be the fingerprint generation function, mapping each key to an n -bit value. For a given set of keys \mathcal{U} , we can compute the fingerprint array \mathcal{H} as:

$$\mathcal{H} = \bigcup_{k \in \mathcal{U}} \phi(k) = \bigcup_{k \in \mathcal{U}} \left(\bigcup_{j=1}^m \{h_j(f(k))\} \right) \quad (1)$$

Here, $\phi(k)$ computes the set of m locations in \mathcal{H} for each key k in \mathcal{U} . Once \mathcal{H} is constructed, we can perform a membership check as:

$$\text{Member}(x) = \begin{cases} \text{true}, & \bigoplus_{j=1}^m \mathcal{H}[h_j(f(x))] = f(x) \\ \text{false}, & \text{otherwise} \end{cases} \quad (2)$$

where, $\bigoplus_{j=1}^m \mathcal{H}[\cdot]$ represents the bitwise XOR operation performed on the array values of \mathcal{H} , indicated by the hash functions $h_j(f(x))$. The *Member*(\cdot) function returns true if the result of the XOR operation over \mathcal{H} matches the fingerprint $f(x)$, suggesting that x is likely a member of the set, and false in all other occasions. Note that while computing a large number of hashes may seem daunting, not all hashing algorithms are computationally intensive. For example, BFuse use MurmurHash3 Appleby (2016), which is computationally efficient and exhibits exceptional properties for hashing large data structures into space-efficient arrays (e.g., uniform hash distribution and randomness).

Stochastic Mask Training. Unlike the thresholding mechanisms Li et al. (2021a); Vallapuram et al. (2022);

Mozaffari et al. (2022) that creates binary masks by clipping mask scores $s \in \mathbb{R}^d$, stochastic mask training Isik et al. (2023b), involves drawing a binary mask $m \in \{0, 1\}^d$ from the underlying mask’s probability θ using the Bernoulli distribution (noted as $m \sim \text{Bern}(\theta)$). To generate θ from the *unbounded* mask scores s , a sigmoid transformation is applied (i.e., $\theta = \text{Sigmoid}(s)$). Hence, m is used during the forward pass to compute the loss $\mathcal{L}(\cdot)$, and θ is subsequently updated through back-propagation. As the values of s remain *unbounded*, it allows for an unbiased estimation of the true aggregate of the local clients’ mask probabilities through Bayesian aggregation Ferreira et al.. Specifically, it refines the global model at round t in federated setting by treating the stochastic mask’s probability $\theta^{g,t}$ as a Beta distribution $\text{Beta}(\alpha_{g,t}, \beta_{g,t})$, with $\alpha_{g,t}$ and $\beta_{g,t}$ initialized to λ_0 . These parameters are updated with the aggregated local binary masks from participating clients (denoted as $\bar{\theta}^{g,t}$), computed as $\alpha_{g,t} = \alpha_{g,t-1} + \bar{\theta}^{g,t}$ and $\beta_{g,t} = \beta_{g,t-1} + K \cdot \mathbf{1}_d - \bar{\theta}^{g,t}$. The aggregated probability mask is then calculated by:

$$\theta^{g,t} = \frac{\alpha_{g,t} - 1}{\alpha_{g,t} + \beta_{g,t} - 2}, \quad (3)$$

where the division is performed element-wise division. For best performance, α and β are periodically reset to $\lambda_0 = 1$ at a rate inverse to the participation rate p Isik et al. (2023b). It’s important to note that while the model’s weight values remain unchanged, the binary mask m selectively activates neurons by element-wise multiplication with the initialized model weights w_{init} , denoted as $w_{k,t} = m^{k,t} \odot w_{\text{init}}$.

3.2 Federated Masked Fine Tuning of Self-Supervised Foundation Models

Overview. Here, we present the general DeltaMask training pipeline (see Figure 2). First, clients initialize a neural network $p_{w_{\text{init}}}$ with the weight vector $w_{\text{init}} = (w_{\text{init},1}, w_{\text{init},2}, \dots, w_{\text{init},d}) \in \mathbb{R}^d$, from the pre-trained foundation model. The weight vector w_{init} is kept fixed and never modified during training. DeltaMask collaboratively trains a probabilistic mask $\theta \in [0, 1]^d$, such that the function $\mathcal{L}_{\dot{W}}$ minimize its error rate on a given downstream task ($\dot{W} = m \odot w_{\text{init}}$). Specifically, at every federated round t , the server samples a set K_t participants ($|K_t|=K$ out of N clients), which individually train their local probability masks $\theta^{k,t}$ on their locally stored datasets D^k , each composed of $|D_k|$ samples.

Instead of communicating the stochastic binary mask m , we significantly reduce the required bits-per-parameter (bpp) during the training process by solely communicating the subsequent key updates (indicated as position indexes set Δ) between the received and trained mask. In particular, we efficiently represent Δ using probabilistic filters and transmit the fingerprint set \mathcal{H} to the server via means of a single gray-scaled image. On server-side reconstruction of clients masks $m^{k,t}$ is feasible via fast membership check using the probabilistic filter. These local masks are then aggregated by the server to complete the t_{th} round.

Compressing Mask Updates. Our approach utilizes a local training scheme for probability masks, inspired by the success of recent methods Zhou et al. (2020); Isik et al. (2023b). In brief, clients receive a global probability mask $\theta^{g,t-1}$ at round t , where each client k performs local training and updates the mask via back-propagation. To satisfy $\theta^{k,t} \in [0, 1]^d$ without clipping, we apply a sigmoid operation over the mask’s *unbounded* mask scores $s \in \mathbb{R}^d$. Then, clients can utilize a binary mask $m^{k,t}$, i.e, sampled from $\text{Bern}(\theta^{k,t})$ and aim to minimize $\mathcal{L}(p_{w_{k,t}}, D^k)$ over their locally stored data, D^k , after which they back-propagate to update their mask scores.

To enable ultra-low bitrate levels, DeltaMask leverages the inherent sparsity in consecutive mask updates in subsequent federated rounds. For a given round t , we deterministically sample a binary mask $m^{g,t-1}$ from the received mask distribution, $\text{Bern}(\theta^{g,t-1})$ using a publicly shared *seed*. This ensures uniformity of the generated binary mask among all clients ($m_i^{g,t-1} = m_j^{g,t-1}$ for any $i, j \in K$). Instead of communicating $m^{k,t}$ (or a compressed version of it), we catalog the index positions of differences between $m^{g,t-1}$ and $m^{k,t}$ to create a set of index differences, denoted as $\Delta^{k,t}$. As the mask updates sparsity progressively increase during training, we introduce a top_κ ranking that selects $\kappa\%$ of $\Delta^{k,t}$ based on their relative entropy between the received and the updated probability masks. As a result, we bring a notion of importance sampling into the communication

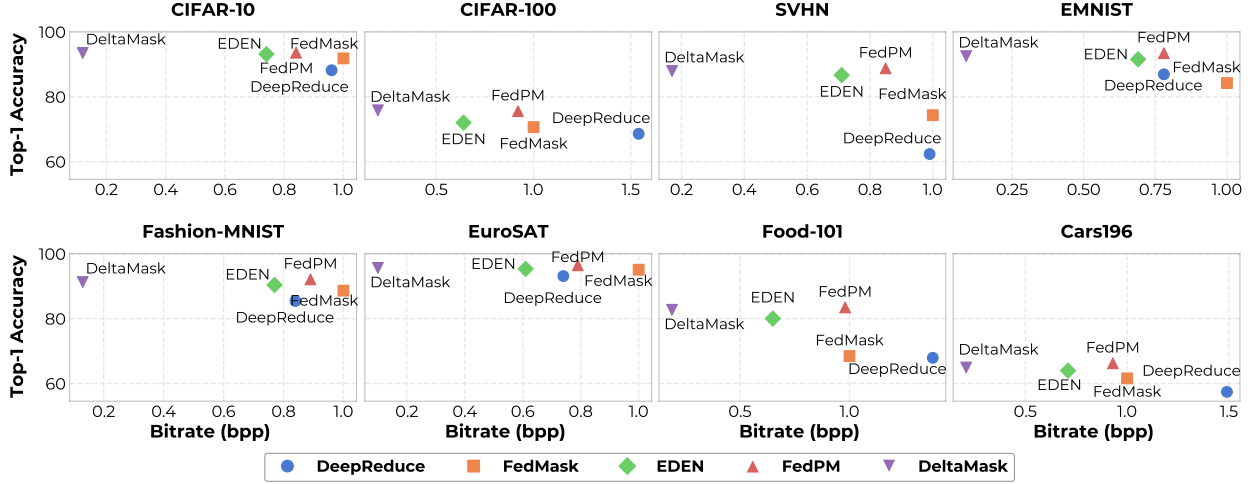


Figure 3: Performance evaluation of DeltaMask (**Ours**) in terms of average bitrate (bits-per-parameter) during FL training using $Dir(10)$ over classes ($C_p \approx 1.0$ / **IID settings**) for CLIP ViT-B/32. Federated parameters are set to $N=30$, $R=100$, $\rho=1$, and $E=1$. Detailed performance metrics, including comparison with Linear Probing and Fine-tuning, can be found in Table 2 of Appendix C.2

scheme, similar to Isik et al. (2023a); Chatterjee and Diaconis (2017); Havasi et al. (2018), helping minimize the distributed mean estimation error under low bitrate regimes. It yields essential updates in early training stages while allowing to convey more detailed information of $m^{k,t}$ without disproportionately increasing the bitrate due to the increasing sparsity of mask differences. Using Kullback–Leibler (KL) divergence as a measure of entropy, $\Delta^{k,t}$ is formally defined as:

$$\Delta^{k,t} = \underset{KL(\theta^{k,t}, \theta^{g,t-1})}{Sort} \left\{ i \mid m_i^{g,t-1} \neq m_i^{k,t}, \forall i \in d \right\} [1 : K], \quad (4)$$

where d is the dimension of the probability mask m , and K represents the number of elements to be retained in the sorted set, determined as $\kappa\%$ of $|D_k|$.

Next, we utilize an 4-wise *binary fuse filters* with 8-bit per entry (noted as BFuse8) to extract a fingerprint array $\mathcal{H}^{k,t}$ from $\Delta^{k,t}$, following Eq. 1. By doing so, we essentially transition from 32-bit indexes to ≈ 8 -bit hashed entries. We further encode the fingerprints set $\mathcal{H}^{k,t}$ into a gray-scale image using lossless image compression techniques $\Psi(\cdot)$, such as DEFLATE, reducing the bitrate further by taking advantage of possible non-uniform distributions of entries across the fingerprints locations. The resulting image, denoted as $A_{k,t}$, now efficiently encapsulates the mask updates in a visual and compressed format, suitable for transmission to the server.

Bayesian Aggregation of Compressed Masks. Once the local training at round t is completed, the server needs to form a new global probability mask from the received clients’ gray-scale images, $A_{k,t}$. Specifically, for each client k , server first decompress the gray-scale image to the extract $\mathcal{H}^{k,t}$ using $\Psi^{-1}(A_{k,t})$ and reconstruct the client’s *original* probabilistic filter, $BFuse8_k$. The indexes of updates from prior server mask $m^{g,t-1}$ for client k can now be estimated via a membership query across all possible indexes of $m^{g,t-1}$, as follows:

$$\hat{\Delta}^{k,t} = \{i \mid \text{Member}(i) = \text{true}, \forall i \in d\} \quad (5)$$

The clients’ stochastic binary sample mask $m^{k,t}$ from $\text{Bern}(\theta^{k,t})$ can be constructed by a simple “bit-flip” of $m^{g,t-1}$ in the positions derived from $\hat{\Delta}^{k,t}$. Now, server can compute the estimated aggregated probability mask $\bar{\theta}^{g,t} = \frac{1}{K} \sum_{k \in K} m^{k,t}$, which is an unbiased estimation of the underlying probability mask $\theta^{g,t} = \frac{1}{K} \sum_{k \in K} \theta^{k,t}$ using Isik et al. (2023b); Ferreira et al. or a similar strategy. Furthermore, DeltaMask has a bounded estimation error (proof given in Appendix B) defined as:

$$\mathbb{E}_{M^{k,t} \sim \text{Bern}(\theta^{k,t}) \forall k \in K} \left[\left\| \theta^{g,t} - \bar{\theta}^{g,t} \right\|_2^2 \right] \leq \frac{d}{4K} \quad (6)$$

In contrast to related approaches, such as FedPM [Isik et al. \(2023b\)](#) and HideNseek [Vallapuram et al. \(2022\)](#), our method enables better control over the model generalization versus bitrate bpp during FL training stage. While we primarily focus on 8-bit per entry (bpe) in our probabilistic filters, we provide analysis of bpe in Section 5.4. We also provide a complete algorithm in Appendix A.

3.3 Weight Initialization

The neural network $p_{w_{\text{init}}}$ is initialized using weights $w_{\text{init}} = (w_{\text{init},1}, w_{\text{init},2}, \dots, w_{\text{init},d}) \in \mathbb{R}^d$ derived from a pre-trained foundation model, yet, the classification head for downstream tasks is randomly initialized. This means that while the pre-trained backbone offers high-quality features useful across various tasks, the randomly initialized classifier head significantly influences the model’s overall performance. Prior research has sampled weights from a uniform distribution around the Kaiming initialization to find highly-performing subnetworks on randomly initialized network [Isik et al. \(2023b\)](#); [Zhou et al. \(2020\)](#); [Ramanujan et al. \(2020\)](#); [Zhou et al. \(2020\)](#). However, as we focus on pre-trained models, we allow the classification head to adapt during a single round of linear probing, where the rest of the model remains frozen. This yields more stable results and rapid convergence. For a fair comparison, we employ identical weights initialization methods across all considered baselines. We also investigate scenarios with extremely low bitrates, where, linear probing is not feasible in Appendix C.5.

3.4 Privacy

In FL, protecting privacy is essential, as model updates might inadvertently expose client data [Wang et al. \(2020\)](#). Our approach employs probabilistic filters like binary fuse filters for stochastic mask updates, enhancing data privacy due to their reliance on multiple hashing operations sensitive to initial conditions. Securely setting an initial *seed* via a secure channel with the server, such as public-private key pairing, helps prevent eavesdropping on clients’ updates. While providing absolute privacy guarantees is not the primary objective of De1taMask, its hashing operations inherently boost privacy, a beneficial side effect. We leave further exploration of this to future work.

4 Experiment Setup

Datasets and FL Settings. We conduct experiments across 8 diverse image classification datasets, namely CIFAR-10 [Krizhevsky \(2009\)](#), CIFAR-100 [Krizhevsky \(2009\)](#), SVHN [Netzer et al. \(2011\)](#), EMNIST [Cohen et al. \(2017\)](#) with 49 classes, Fashion-MNIST [Xiao et al. \(2017\)](#), EuroSAT [Helber et al. \(2017\)](#) with 10 classes, Food-101 [Bossard et al. \(2014\)](#) with 101 classes, and Cars196 [Krause et al. \(2013\)](#) with 196 classes. We utilize popular ViT architectures pre-trained in self-supervised manner, such as CLIP [Radford et al. \(2021\)](#), DINOv2 [Oquab et al. \(2023\)](#), where, we learn a mask for the last five transformer blocks and keep all prior blocks frozen, similar to [Zhao et al. \(2020\)](#). In all experiments with CLIP, we use CLIP ViT-B/32, unless stated otherwise. Apart from ViT architectures, we also evaluate convolution-based model, namely ConvMixer-768/32 [Trockman and Kolter \(2022\)](#), where mask is learned for the last five convolutional blocks, similar to ViT.

For our data splitting procedure, we utilized Dirichlet distribution over classes, denoted as $Dir(a)$, where a refers to the distribution concentration, following [Li et al. \(2021b\)](#). For IID experiments, we fix $a=10$, essentially setting the class distribution per client (referred to as C_p) to ≈ 1.0 (examples from all classes are available across clients), while for non-IID settings, we set $a=0.1$, which results in a $C_p \approx 0.2$. In each round, clients perform a single local training step ($E=1$) and we use a cosine scheduler for top_κ mechanism starting

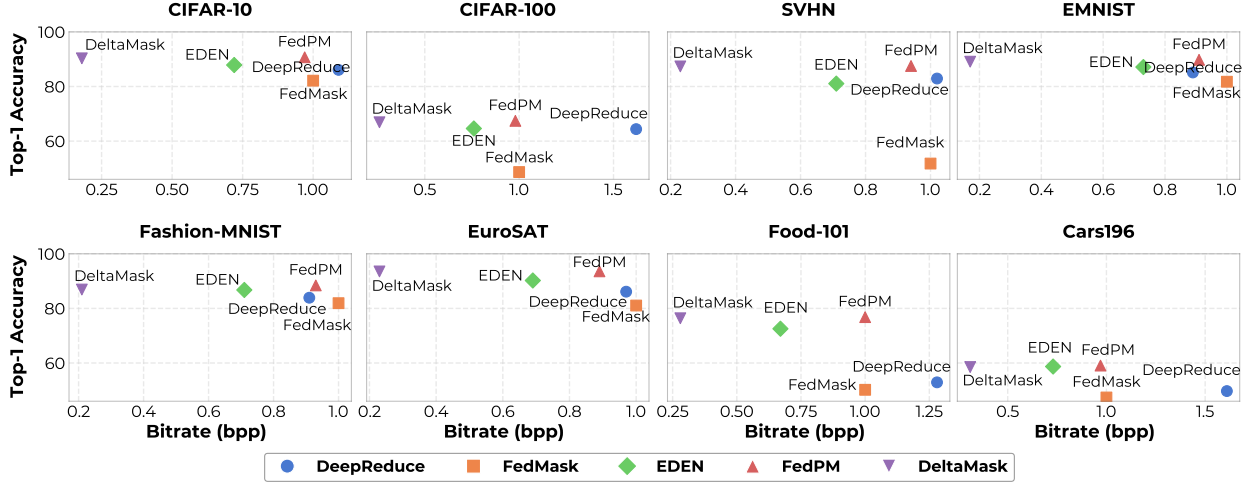


Figure 4: Performance evaluation of DeltaMask (**Ours**) in terms of average bitrate (bits-per-parameter) during FL training using $Dir(0.1)$ over classes ($C_p \approx 0.2$ / **non-IID settings**) for CLIP ViT-B/32. Federated parameters are set to $N=30$, $R=300$, $\rho=0.2$, and $E=1$. Detailed performance metrics, including comparison with Linear Probing and Fine-tuning, can be found in Table 3 of Appendix C.3

from $\kappa=0.8$. Due to limited space, we provide additional details of the experimental setup in Appendix C.1.

Baselines. We evaluate DeltaMask in terms of accuracy, bitrate (bits-per-parameters), computational complexity and total volume of communicated data between client and server. In our baselines, we include both fine-tuning and linear probing, where the latter involves training a classifier on top of a frozen backbone architecture. From the domain of gradient compression techniques, we incorporate EDEN Vargaftik et al. (2022), DRIVE Vargaftik et al. (2021), QSGD Alistarh et al. (2017), and FedCode Khalilian et al. (2023) into our evaluation. Additionally, we consider DeepReduce Kostopoulou et al. (2021) as a baseline owing to its analogous use of bloom filter-based compressor. From the threshold-based masking strategies in FL, we compare against FedMask Li et al. (2021a), albeit without its initial pruning phase (typically used for personalization), aligning it more closely with FedPM Isik et al. (2023b). Leveraging concepts from stochastic masking, we include FedPM Isik et al. (2023b) in our set of baselines to accurately assess the bitrate improvements offered by DeltaMask. For a rigorous evaluation, we follow the weight initialization scheme of Section 3.3 across all our baselines, where we use pre-trained weights from HuggingFace for each backbone architecture. We perform our experiments using Flower framework Beutel et al. (2020) and report the results averaged over three runs.

5 Results

5.1 Bitrate-Accuracy Trade-Off

IID Data Split. Here, we focus on IID data distribution, with the number of clients (N) set to 30 and full client participation ($\rho=1$). As depicted in Figure 3, DeltaMask achieves significant reductions in communication costs compared to the considered baselines - consistently across all datasets. Among the baselines, EDEN requires the least bandwidth, while FedPM attains the highest accuracy; nevertheless, DeltaMask reliably matches the accuracy of FedPM. This notable improvement in bitrate over FedPM indicates that mask updates entail significant overhead. Transmitting only essential information via binary fuse filters leads to considerable reductions in bpp (up to approximately $9\times$ less without compromising on model accuracy. In comparison to DeepReduce — which utilizes Bloom filters to transmit the updates — our method underscores

Table 1: Evaluation of DeltaMask using $Dir(10.0)$ over classes ($C_p \approx 1.0$ / IID settings) across architectures and pre-training strategies.

Metric	CLIP ViT-B/32	CLIP ViT-L/14	DINOv2-Base	DINOv2-Small	ConvMixer-768/32
Fine-tuning	77.35 ± 0.009	89.07 ± 0.012	75.01 ± 0.007	65.55 ± 0.019	78.52 ± 0.009
DeltaMask (Ours)	75.82 ± 0.023	89.48 ± 0.031	73.36 ± 0.027	63.01 ± 0.033	75.31 ± 0.021
Avg. bpp	0.207 ± 0.001	0.225 ± 0.002	0.197 ± 0.001	0.214 ± 0.001	0.251 ± 0.001

the importance of accurate mask reconstruction, as Bloom filters are prone to a higher false positive rate for the same number of hash functions and bits per entry. Further experimental results under conditions of low client participation in IID settings are presented in Appendix C.2, which continue to demonstrate the advantages of DeltaMask in reducing bitrate.

Non-IID Data Split. We now evaluate in a more realistic federated setting, where clients’ data follow a non-IID distribution using $Dir(0.1)$ over classes ($C_p \approx 0.2$). Furthermore, the number of clients (N) set to 30, while we consider partial participation with $\rho=0.2$ (meaning that in each round $\rho \cdot N = 6$ clients are randomly selected). This represents a challenging and realistic scenario, where clients have limited network resources and their data generation processes differ drastically, leading to different data distribution. From Figure 4, we notice similar gains over the baselines as the IID experiments presented in Figure 3; in that DeltaMask can maintain a learning procedure that results in better generalizable model, despite having up to a 6-fold reduction in the communication cost. Furthermore, the Bayesian aggregation mechanism, as presented in Eq. 3, is pivotal in achieving high accuracy when $\rho < 1$ under non-IID settings; evident from the increase in performance of DeepReduce compared to FedMask that performs poorly across all datasets. Note that in IID setting with full client participation, this behavior was reversed. We provide additional experiments under a similar non-IID setting with full client participation in Appendix C.3, where the superiority of DeltaMask in terms of bitrate reduction is evident.

5.2 Evaluating Improvements in Data Volume and Computational Cost

We evaluate the impact of DeltaMask on computational resources at both client and server levels, as well as the communication efficiency relative to the total data volume transmitted. For this, we perform experiments using CLIP on CIFAR-100 with $N=10$, and measure the encoding and decoding times for various gradient compression schemes: EDEN, DRIVE, and FedCode. Additionally, DeepReduce is included for comparison with DeltaMask in terms of efficiency against Bloom-based compression. From masking approaches, we include FedMask and FedPM, omitting their arithmetic encoding step to simplify computational complexity and ensure comparable execution times. All tests are conducted on a CPU, excluding aggregation in decoding time measurements. Data volume is normalized against full fine-tuning size, and we report the necessary volume to reach within 1% of peak accuracy, effectively combining communication efficiency with convergence speed analysis.

Among the evaluated methods in Figure 7, FedCode is the most communication-efficient in terms of data volume; yet, it suffers from longer encoding times and has the lowest model performance across baselines. Additionally, we notice that DeepReduce, utilizing a Bloom-based compressor, struggles with scalability due to longer execution times; in contrast, while DeltaMask offer significant improvements in filter construction and query times. FedMask and FedPM offer a compromise between data volume and execution time, with FedPM notably leading in accuracy among all approaches. Surprisingly, DeltaMask, while using slightly more data than FedCode, provides quicker encoding, critical for devices with limited resources, and matches the high accuracy of FedPM with significantly less data communicated. This positions DeltaMask as an effective choice for environments with computational and communication constraints. To further emphasize this point, we perform an analysis on multiple common edge devices utilized on edge in Appendix C.4.

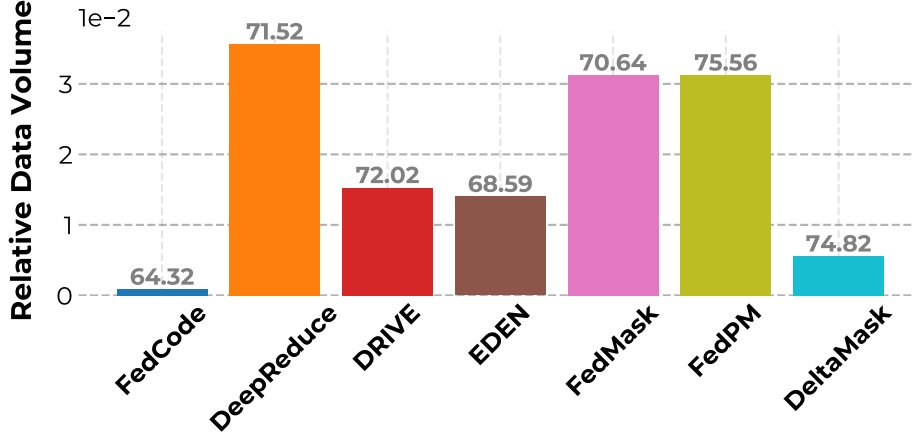


Figure 5: Relative Data Volume against fine-tuning size.

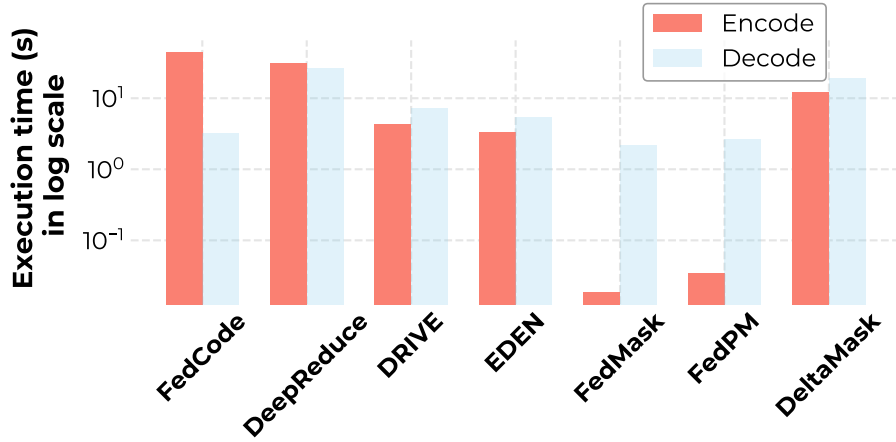


Figure 6: Encode/Decode run time on CPU.

Figure 7: Performance evaluation of DeltaMask (**Ours**) in terms of (a) data volume and (b) encoding/decoding time (with baselines), required for CLIP ViT-B/32 to reach within 1% of peak performance on CIFAR-100. Data volume is normalized over full fine-tuning data size.

5.3 Generalization across Neural Architectures and Pre-training Strategies

Next, we evaluate DeltaMask ability to work across various neural architectures pre-trained in a different self-supervised manner. We train masks for downstream task adaptation in a communication-constrained FL environment. For this, we perform experiments with $N=10$ on additional (larger) ViT architectures, namely CLIP-Large and DINOv2-Large, as well as a pure convolution-based architecture, ConvMixer-768/32 on CIFAR-100 as a downstream classification task. In all experiments, we mask the last 5 blocks, as discussed in Section 4. From Table 1, DeltaMask demonstrates robust adaptability across diverse pre-trained architectures in a FL setup with communication constraints. Notably, DeltaMask performance on large ViT architectures yield accuracies near those of fine-tuning, notably with CLIP ViT-L/14 slightly surpassing it. This is significant, considering the communication efficiency depicted by the average bitrate, which remains close to 0.2 bpp across all architectures. ConvMixer-768/32 also adapts well with DeltaMask, showing a modest accuracy reduction while meeting communication constraints. These results reinforce our method’s suitability across diverse architectures, allowing for communication-efficient downstream task adaptation of FMs in a federated setting.

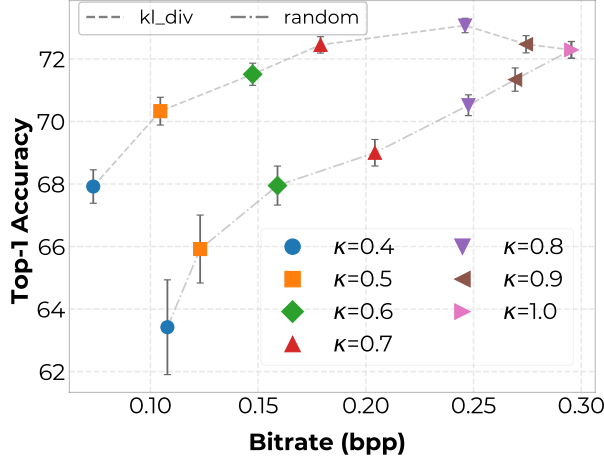


Figure 8: Top- κ percentages

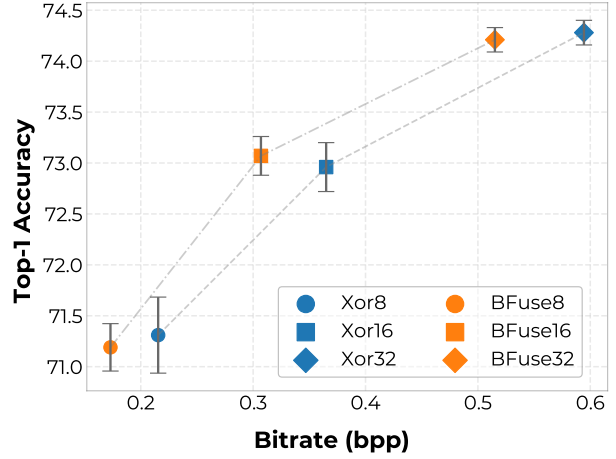


Figure 9: Probabilistic filters

Figure 10: Impact of top- κ mechanism and probabilistic filter choice in DeltaMask performance. Experiments performed in CIFAR-100 using Dir(10) over classes ($C_p \approx 1.0$ / IID settings). Federated parameters are set to $N=10$, $R=100$, $\rho=1$ and $E=1$.

5.4 Adjusting Bitrate in DeltaMask

Now, we do ablation of fundamental components in DeltaMask: the mechanism sorting the positions of mask updates indexes and our choice of probabilistic filter, assessing the impact of these components on the model’s final accuracy and bitrate. For this, we conduct experiments using CLIP ViT-B/32 with $N=10$ under full participation. In Figure 8, we compare our entropy-based top_κ sorting with a naive random sampling mechanism. We notice a consistent gap in performance between these approaches, underscoring the pivotal role of importance sampling in achieving generalization, similar to Isik et al. (2023a). Surprisingly, increasing κ does not linearly enhance accuracy, with the best results observed at $\kappa=0.8$, beyond which performance diminishes. This suggests that our top_κ approach effectively filters out noise inherent in the stochastic binary mask sampling mechanism by prioritizing updates with higher certainty (i.e., higher probability), while also benefiting from a reduced bitrate due to transmitting less data.

Lastly, we evaluate the performance of various probabilistic filters, focusing on how variations in bits-per-entry (bpe), ranging from 8 to 32 bits, affect the false positive rate. Our analysis includes binary fuse filters (BFuse) and XoR Graf and Lemire (2020) filters, the latter operating under the same foundational principles but being slightly less space-efficient. Figure 9 demonstrates that BFuse filters generally surpass XoR filters in reducing bitrate without compromising model accuracy, a consistency observed across all experiments. More importantly, we demonstrate that DeltaMask enables an adjustable bitrate based on the bpe selection within the probabilistic filter, offering a potential solution to address the resource heterogeneity among clients in FL.

6 Conclusions

We introduce DeltaMask a FL technique for efficiently fine-tuning FMs under low bitrate constraints by utilizing stochastic masking instead of conventional fine-tuning and leveraging probabilistic filters for communicating subsequent clients’ mask updates. Our evaluation demonstrates DeltaMask’s effectiveness across a broad range of datasets and FMs, where it achieves significant communication reductions with performance similar to traditional fine-tuning.

Limitations and Broader Impacts. While we showed that DeltaMask, when combined with FedPM, greatly re-

duces communication overhead, its adaptation to other stochastic FL frameworks for similar gains has not been explored within the scope of this study. While DeltaMask shows promising performance in communication-efficiency, aspects like fairness and privacy in FL still require further exploration and validation.

Acknowledgement

Vasileios Tsouvalas research is partially funded by the DAIS project, which has received funding from KDTJU under grant agreement No. 101007273.

References

- Alham Fikri Aji and Kenneth Heafield. Sparse communication for distributed gradient descent. In *Proceedings of the 2017 Conference on Empirical Methods in Natural Language Processing*. Association for Computational Linguistics, 2017. doi: 10.18653/v1/d17-1045. URL <https://doi.org/10.18653/v1/d17-1045>.
- Maxwell Mbabilla Aladago and Lorenzo Torresani. Slot machines: Discovering winning combinations of random weights in neural networks, 2021.
- Dan Alistarh, Demjan Grubic, Jerry Li, Ryota Tomioka, and Milan Vojnovic. Qsgd: Communication-efficient sgd via gradient quantization and encoding, 2017.
- Austin Appleby. Murmurhash3. <https://github.com/aappleby/smhasher/wiki/MurmurHash3>, 2016. Accessed: 13/11/2023.
- Daniel J Beutel, Taner Topal, Akhil Mathur, Xinchu Qiu, Titouan Parcollet, and Nicholas D Lane. Flower: A friendly federated learning research framework. *arXiv preprint arXiv:2007.14390*, 2020.
- Lukas Bossard, Matthieu Guillaumin, and Luc Van Gool. Food-101 – mining discriminative components with random forests. In *European Conference on Computer Vision*, 2014.
- Sourav Chatterjee and Persi Diaconis. The sample size required in importance sampling, 2017.
- Wenlin Chen, Samuel Horvath, and Peter Richtarik. Optimal client sampling for federated learning, 2022.
- Gregory Cohen, Saeed Afshar, Jonathan Tapson, and André van Schaik. Emnist: an extension of mnist to handwritten letters, 2017.
- Mostafa Dehghani, Josip Djolonga, Basil Mustafa, Piotr Padlewski, Jonathan Heek, Justin Gilmer, Andreas Steiner, Mathilde Caron, Robert Geirhos, Ibrahim Alabdulmohsin, Rodolphe Jenatton, Lucas Beyer, Michael Tschannen, Anurag Arnab, Xiao Wang, Carlos Riquelme, Matthias Minderer, Joan Puigcerver, Utku Evci, Manoj Kumar, Sjoerd van Steenkiste, Gamaleldin F. Elsayed, Aravindh Mahendran, Fisher Yu, Avital Oliver, Fantine Huot, Jasmijn Bastings, Mark Patrick Collier, Alexey Gritsenko, Vighnesh Birodkar, Cristina Vasconcelos, Yi Tay, Thomas Mensink, Alexander Kolesnikov, Filip Pavetić, Dustin Tran, Thomas Kipf, Mario Lučić, Xiaohua Zhai, Daniel Keysers, Jeremiah Harmsen, and Neil Houlsby. Scaling vision transformers to 22 billion parameters, 2023.
- Paulo Abelha Ferreira, Pablo Nascimento da Silva, Vinicius Gottin, Roberto Stelling, and Tiago Calmon. Bayesian signsgd optimizer for federated learning.
- Jonathan Frankle and Michael Carbin. The lottery ticket hypothesis: Finding sparse, trainable neural networks, 2019.
- Thomas Mueller Graf and Daniel Lemire. Xor filters: Faster and smaller than bloom and cuckoo filters. *ACM Journal of Experimental Algorithmics*, 25:1–16, March 2020. ISSN 1084-6654. doi: 10.1145/3376122. URL <http://dx.doi.org/10.1145/3376122>.

- Thomas Mueller Graf and Daniel Lemire. Binary fuse filters: Fast and smaller than xor filters. *ACM J. Exp. Algorithmics*, 27, mar 2022. ISSN 1084-6654. doi: 10.1145/3510449. URL <https://doi.org/10.1145/3510449>.
- Marton Havasi, Robert Peharz, and José Miguel Hernández-Lobato. Minimal random code learning: Getting bits back from compressed model parameters, 2018.
- Patrick Helber, Benjamin Bischke, Andreas Dengel, and Damian Borth. Eurosat: A novel dataset and deep learning benchmark for land use and land cover classification, 2017.
- Berivan Isik, Francesco Pase, Deniz Gunduz, Sanmi Koyejo, Tsachy Weissman, and Michele Zorzi. Communication-efficient federated learning through importance sampling, 2023a.
- Berivan Isik, Francesco Pase, Deniz Gunduz, Tsachy Weissman, and Michele Zorzi. Sparse random networks for communication-efficient federated learning, 2023b.
- Saeed Khalilian, Vasileios Tsouvalas, Tanir Ozcelebi, and Nirvana Meratnia. Fedcode: Communication-efficient federated learning via transferring codebooks, 2023.
- Jakub Konečný, H. Brendan McMahan, Felix X. Yu, Peter Richtarik, Ananda Theertha Suresh, and Dave Bacon. Federated learning: Strategies for improving communication efficiency. In *NIPS Workshop on Private Multi-Party Machine Learning*, 2016. URL <https://arxiv.org/abs/1610.05492>.
- Kelly Kostopoulou, Hang Xu, Aritra Dutta, Xin Li, Alexandros Ntoulas, and Panos Kalnis. Deepreduce: A sparse-tensor communication framework for distributed deep learning, 2021.
- Jonathan Krause, Michael Stark, Jia Deng, and Li Fei-Fei. 3d object representations for fine-grained categorization. In *2013 IEEE International Conference on Computer Vision Workshops*, pages 554–561, 2013. doi: 10.1109/ICCVW.2013.77.
- Alex Krizhevsky. Learning multiple layers of features from tiny images. Technical report, 2009.
- Ang Li, Jingwei Sun, Binghui Wang, Lin Duan, Sicheng Li, Yiran Chen, and Hai Li. Lotteryfl: Personalized and communication-efficient federated learning with lottery ticket hypothesis on non-iid datasets, 2020.
- Ang Li, Jingwei Sun, Xiao Zeng, Mi Zhang, Hai Li, and Yiran Chen. Fedmask: Joint computation and communication-efficient personalized federated learning via heterogeneous masking. *SenSys '21*, page 42–55, New York, NY, USA, 2021a. Association for Computing Machinery. ISBN 9781450390972. doi: 10.1145/3485730.3485929. URL <https://doi.org/10.1145/3485730.3485929>.
- Qinbin Li, Yiqun Diao, Quan Chen, and Bingsheng He. Federated learning on non-iid data silos: An experimental study, 2021b.
- Yujun Lin, Song Han, Huizi Mao, Yu Wang, and William J. Dally. Deep gradient compression: Reducing the communication bandwidth for distributed training, 2020.
- Arun Mallya, Dillon Davis, and Svetlana Lazebnik. Piggyback: Adapting a single network to multiple tasks by learning to mask weights, 2018.
- Brendan McMahan, Eider Moore, Daniel Ramage, Seth Hampson, and Blaise Agüera y Arcas. Communication-Efficient Learning of Deep Networks from Decentralized Data. In Aarti Singh and Jerry Zhu, editors, *Proceedings of the 20th International Conference on Artificial Intelligence and Statistics*, volume 54 of *Proceedings of Machine Learning Research*, pages 1273–1282. PMLR, 20–22 Apr 2017. URL <https://proceedings.mlr.press/v54/mcmahan17a.html>.
- Amirkeivan Mohtashami, Martin Jaggi, and Sebastian U. Stich. Masked training of neural networks with partial gradients, 2022.
- Hamid Mozaffari, Virat Shejwalkar, and Amir Houmansadr. Frl: Federated rank learning, 2022.

- Yuval Netzer, Tao Wang, Adam Coates, Alessandro Bissacco, Bo Wu, and Andrew Y Ng. Reading digits in natural images with unsupervised feature learning. 2011.
- Maxime Oquab, Timothée Darcet, Théo Moutakanni, Huy Vo, Marc Szafraniec, Vasil Khalidov, Pierre Fernandez, Daniel Haziza, Francisco Massa, Alaaeldin El-Nouby, Mahmoud Assran, Nicolas Ballas, Wojciech Galuba, Russell Howes, Po-Yao Huang, Shang-Wen Li, Ishan Misra, Michael Rabbat, Vasu Sharma, Gabriel Synnaeve, Hu Xu, Hervé Jegou, Julien Mairal, Patrick Labatut, Armand Joulin, and Piotr Bojanowski. Dinov2: Learning robust visual features without supervision, 2023.
- Alec Radford, Jong Wook Kim, Chris Hallacy, A. Ramesh, Gabriel Goh, Sandhini Agarwal, Girish Sastry, Amanda Askell, Pamela Mishkin, Jack Clark, Gretchen Krueger, and Ilya Sutskever. Learning transferable visual models from natural language supervision. In *ICML*, 2021.
- Vivek Ramanujan, Mitchell Wortsman, Aniruddha Kembhavi, Ali Farhadi, and Mohammad Rastegari. What’s hidden in a randomly weighted neural network?, 2020.
- Sashank Reddi, Zachary Charles, Manzil Zaheer, Zachary Garrett, Keith Rush, Jakub Konečný, Sanjiv Kumar, and H. Brendan McMahan. Adaptive federated optimization, 2021.
- J. Rissanen and G. G. Langdon. Arithmetic coding. *IBM Journal of Research and Development*, 23(2):149–162, 1979. doi: 10.1147/rd.232.0149.
- Aliaksandra Shysheya, John Bronskill, Massimiliano Patacchiola, Sebastian Nowozin, and Richard E Turner. Fit: Parameter efficient few-shot transfer learning for personalized and federated image classification. *arXiv preprint arXiv:2206.08671*, 2022.
- Asher Trockman and J. Zico Kolter. Patches are all you need?, 2022.
- Anish K. Vallapuram, Pengyuan Zhou, Young D. Kwon, Lik Hang Lee, Hengwei Xu, and Pan Hui. Hidenseek: Federated lottery ticket via server-side pruning and sign supermask, 2022.
- Shay Vargaftik, Ran Ben Basat, Amit Portnoy, Gal Mendelson, Yaniv Ben-Itzhak, and Michael Mitzenmacher. Drive: One-bit distributed mean estimation, 2021.
- Shay Vargaftik, Ran Ben Basat, Amit Portnoy, Gal Mendelson, Yaniv Ben Itzhak, and Michael Mitzenmacher. EDEN: Communication-efficient and robust distributed mean estimation for federated learning. In Kamalika Chaudhuri, Stefanie Jegelka, Le Song, Csaba Szepesvari, Gang Niu, and Sivan Sabato, editors, *Proceedings of the 39th International Conference on Machine Learning*, volume 162 of *Proceedings of Machine Learning Research*, pages 21984–22014. PMLR, 17–23 Jul 2022. URL <https://proceedings.mlr.press/v162/vargaftik22a.html>.
- Hongyi Wang, Kartik Sreenivasan, Shashank Rajput, Harit Vishwakarma, Saurabh Agarwal, Jy-yong Sohn, Kangwook Lee, and Dimitris Papailiopoulos. Attack of the tails: Yes, you really can backdoor federated learning. In H. Larochelle, M. Ranzato, R. Hadsell, M.F. Balcan, and H. Lin, editors, *Advances in Neural Information Processing Systems*, volume 33, pages 16070–16084. Curran Associates, Inc., 2020. URL https://proceedings.neurips.cc/paper_files/paper/2020/file/b8ffa41d4e492f0fad2f13e29e1762eb-Paper.pdf.
- Han Xiao, Kashif Rasul, and Roland Vollgraf. Fashion-mnist: a novel image dataset for benchmarking machine learning algorithms. *CoRR*, abs/1708.07747, 2017.
- Mengjie Zhao, Tao Lin, Fei Mi, Martin Jaggi, and Hinrich Schütze. Masking as an efficient alternative to finetuning for pretrained language models. In Bonnie Webber, Trevor Cohn, Yulan He, and Yang Liu, editors, *Proceedings of the 2020 Conference on Empirical Methods in Natural Language Processing (EMNLP)*, pages 2226–2241, Online, November 2020. Association for Computational Linguistics. doi: 10.18653/v1/2020.emnlp-main.174. URL <https://aclanthology.org/2020.emnlp-main.174>.
- Hattie Zhou, Janice Lan, Rosanne Liu, and Jason Yosinski. Deconstructing lottery tickets: Zeros, signs, and the supermask, 2020.

A DeltaMask Algorithm

We provide the pseudocode for DeltaMask in Algorithm 1. For completeness, we also provide the Bayesian Aggregation of compressed masks in Algorithm 2.

Algorithm 1 DeltaMask

```

1: Server initialize global model  $G$  with pretrained model weights  $w_{\text{init}}$ .
2: Server initialize mask weights  $\theta^{g,0} \in \mathbf{R}^d$  and Beta priors  $\alpha^{g,0} = \beta^{g,0} = \lambda_0$ .
3: for  $r = 1, \dots, R$  do
4:   Randomly select  $K$  clients to participate in round  $t$ 
5:   for each client  $k \in K$  in parallel do
6:     Sample binary server mask  $m^{g,t-1} \sim \text{Bern}_{t-1}(\theta^{g,t-1})$ 
7:      $\theta^{k,t} \leftarrow \text{ClientUpdate}(\theta^{g,t-1})$ 
8:     Sample binary mask  $m^{k,t} \sim \text{Bern}(\theta^{k,t})$ 
9:      $\Delta'^{k,t} \leftarrow \text{Sort} \{i \mid m^{k,t} \neq m^{g,t-1}\}_{i \in d} [1 : K]$   $\triangleright$  // See Equation 4
10:     $\mathcal{H}^{k,t} \leftarrow \bigcup_{i \in \Delta'^{k,t}} \phi(i)$   $\triangleright$  // See Equation 1
11:     $\text{PNG}^{k,t} \leftarrow \Psi(\mathcal{H}^{k,t})$ 
12:  end for
13:  for each client  $k \in K$  do
14:     $\mathcal{H}^{k,t} \leftarrow \Psi^{-1}(\text{PNG}^{k,t})$ 
15:     $\hat{\Delta}'^{k,t} \leftarrow \{i \mid \text{Member}(i) = \text{true}\}_{i \in d}$   $\triangleright$  // See Equation 5
16:     $m^{k,t} \leftarrow m^{g,t-1} \text{XOR } \mathcal{F}$   $\triangleright$  //  $\mathcal{F}$  is 1 in all positions of  $\hat{\Delta}'^{k,t}$  and 0 otherwise
17:  end for
18:   $\theta^{g,t} \leftarrow \text{BayesAgg}(\{m^{k,t}\}_{k \in K}, t, \rho)$ 
19: end for
20:
21: procedure CLIENTUPDATE( $\theta$ )
22:   for epoch  $e = 1, 2, \dots, E$  do
23:     for batch  $b \in \mathcal{D}^k$  do
24:       Sample a binary mask  $m \sim \text{Bern}(\theta)$ 
25:        $\theta \leftarrow \theta - \eta \nabla_{\theta} (\mathcal{L}_{CE}(y, p_{m \odot w_{\text{init}}}(y|x_b)))$ 
26:     end for
27:   end for
28:   return  $\theta$ 
29: end procedure

```

Algorithm 2 BayesAgg

```

1: Inputs: Clients' updates  $\{m_{k,t}\}_{k \in K}$ , federated round  $t$ , and client participation  $\rho$ .
2: Output: Global probability mask  $\theta_{g,t}$ .
3: if  $t \% (\frac{1}{\rho}) = 0$  then
4:    $\alpha_{g,t-1} = \beta_{g,t-1} = \lambda_0$ 
5: end if
6:  $m^{\text{agg},t} \leftarrow \frac{1}{K} \sum_{k \in K} m^{k,t}$ 
7:  $\alpha^{g,t} = \alpha^{g,t-1} + m^{\text{agg},t}$ 
8:  $\beta^{g,t} = \beta^{g,t-1} + K \cdot 1 - m^{\text{agg},t}$ 
9:  $\theta^{g,t} = \frac{\alpha^{g,t}}{\alpha^{g,t} + \beta^{g,t}}$ 
10: return  $\theta^{g,t}$ 

```

B Distributed Mean Estimation Error Analysis

We now provide proof of the upper bound on the estimation error of DeltaMask. Recall that we use probabilistic filters to reconstruct clients' binary masks, $m^{k,t} \sim \text{Bern}(\theta^{k,t})$ on server-side, which introduce an independent (across both clients and mask dimensions) "bit-flip" error probability 2^{-p} (p referring to the false positive rate of the filter). We refer to these reconstructed masks as $m'^{k,t}$. Here, our true mean is $\bar{\theta}^{g,t} = \frac{1}{K} \sum_{k \in K_t} \theta_k^t$, while our estimate is $\hat{\theta}^{g,t} = \frac{1}{K} \sum_{k \in K_t} m'^{k,t}$. Furthermore, we use capital letters to refer to random variables, while small letters refer to their deterministic quantities. We can then compute the error as follows:

$$\mathbb{E}_{M^{k,t} \sim \text{Bern}(\theta^{k,t}) \forall k \in K} \left[\left\| \bar{\theta}^{g,t} - \hat{\theta}^{g,t} \right\|_2^2 \right] = \sum_{i=1}^d \mathbb{E}_{M_i^{k,t} \sim \text{Bern}(\theta_i^{k,t}) \forall k \in K} \left[\left(\bar{\theta}_i^{g,t} - \hat{\theta}_i^{g,t} \right)^2 \right] \quad (7)$$

$$= \sum_{i=1}^d \mathbb{E}_{M_i^{k,t} \sim \text{Bern}(\theta_i^{k,t}) \forall k \in K} \left[\left(\frac{1}{K} \sum_{k \in K} \left(M_i'^{k,t} - \theta_i^{k,t} \right) \right)^2 \right] \quad (8)$$

$$= \frac{1}{K^2} \sum_{i=1}^d \mathbb{E}_{M_i^{k,t} \sim \text{Bern}(\theta_i^{k,t}) \forall k \in K} \left[\left(\sum_{k \in K} \left(M_i'^{k,t} - \theta_i^{k,t} \right) \right)^2 \right] \quad (9)$$

$$= \frac{1}{K^2} \sum_{i=1}^d \sum_{k \in K} \mathbb{E}_{M_i^{k,t} \sim \text{Bern}(\theta_i^{k,t})} \left[\left(M_i'^{k,t} - \theta_i^{k,t} \right)^2 \right] \quad (10)$$

$$= \frac{1}{K^2} \sum_{i=1}^d \sum_{k \in K} \left((1 - 2^{-p}) \theta_i^{k,t} + 2^{-p} (1 - \theta_i^{k,t}) - \theta_i^{k,t} \right)^2 \quad (11)$$

$$= \frac{1}{K^2} \sum_{i=1}^d \sum_{k \in K} \left(2^{-p} - 2 \cdot 2^{-p} \theta_i^{k,t} \right)^2 \quad (12)$$

$$\leq \frac{d}{4K} \quad (13)$$

We begin by expressing the expected squared L^2 norm of the error $\hat{\theta}^{g,t}$ and $\bar{\theta}^{g,t}$ in (7). From (7) to (8), we use the definitions of $\hat{\theta}^{g,t} = \frac{1}{K} \sum_{k \in K_t} m'^{k,t}$ and $\bar{\theta}^{g,t} = \frac{1}{K} \sum_{k \in K_t} \theta_k^t$. To move from (9) to (10), we use the fact that $M_i'^{k,t}$ and $M_i'^{l,t}$ are independent for $k \neq l$; thus the expected value of cross-product terms in the expansion of squared sum of is zero. At (11), we introduce the "bit-flip" error probability 2^{-p} due to the probabilistic filters. Finally, in (13), given that the variance of a Bernoulli random variable is maximized when the probability of success is 0.5, and that the flipping process does not change this maximum possible variance, we concluded that the upper bound of the expected squared error is $\frac{d}{4K}$, where d is the number of dimensions and K is the number of clients.

C Additional Experiments

C.1 Additional Experimental Details

Training Parameters: For our experiments, clients completed 1 local epoch per round with a batch size of 64 and Adam optimizer with a learning rate of 0.1. We adopted Bayesian aggregation, resetting the prior every $\frac{1}{\rho}$ rounds, where ρ is the participation rate (as per Isik et al. (2023b)). In scenarios where ρ is less than 1.0, client selection in each round was randomized. In most experiments, we set κ to 0.8, except for those detailed in Figure 8. We conducted 100 federated rounds for experiments with $\rho=1$ (both IID and non-IID

settings) and increased the number of rounds to 200 and 300 for IID and non-IID experiments, respectively, when $\rho < 1$. Unless otherwise mentioned, we employed CLIP ViT-B/32 for experiments involving CLIP. We perform 3 independent runs and report the average accuracy on test-set in all our experiments.

Baselines Configuration: For FedMask, we set a binary threshold τ (masking with $m_i=1$ if $\theta_i \geq \tau$, and 0 otherwise) in the range $[0.4, 0.6]$ for IID and $[0.2, 0.0]$ for non-IID experiments, aligning with Isik et al. (2023b). In EDEN, a 1-bit gradient compression scheme was used to match the bitrate (bpp) of other baselines. Notably, EDEN’s compression is model-dependent but yields nearly constant bpp reductions across all experiments. From DeepReduce compression, we discard the values’ compression stage (as we deal with binary masks), and utilize only the Bloom filter-based index compression using the $P0$ -policy Kostopoulou et al. (2021). Here, binary masks were learned via stochastic mask training (Isik et al. (2023b)), ensuring operation near the 1 bpp regime and facilitating clear comparison with DeltaMask. For our comparison with FedPM, we use identical settings albeit the compression scheme with probabilistic filters of DeltaMask, to clearly illustrate the benefits of our approach. We conducted our experiments on NVIDIA A10 GPUs on an internal cluster server, using 2 GPUs per one run.

C.2 Additional Experiments in IID settings

In this section, we present additional experiments conducted under IID settings with varying participation rates (ρ). To ensure a fair comparison, we included both Linear Probing, which involves adapting a single linear classifier atop the (frozen) pre-trained model, and full Fine-tuning, wherein only the layers modified in DeltaMask are fine-tuned. In Table 2, apart from report models’ accuracies across tasks, we include the average bpp and accuracy across all tasks for a concise comparison.

Table 2: Performance evaluation of DeltaMask (**Ours**) in terms of average bitrate (bits-per-parameter) during FL training using $Dir(10)$ over classes ($C_p \approx 1.0$ / **IID settings**) for CLIP ViT-B/32. Federated parameters are set to $N=30$ and $E=1$. For $\rho < 1$, clients are randomly selected.

	Method	CIFAR-10	CIFAR-100	SVHN	EMNIST	Fashion-MNIST	EuroSAT	Food-101	Cars196	Avg. Acc	Avg. bpp
$\rho = 0.2$	Linear Probing	92.12 \pm 0.007	67.23 \pm 0.011	59.70 \pm 0.016	89.89 \pm 0.008	89.05 \pm 0.010	94.81 \pm 0.009	67.58 \pm 0.014	59.87 \pm 0.016	77.51	-
	Fine-tuning	94.38 \pm 0.013	76.12 \pm 0.019	91.88 \pm 0.012	94.02 \pm 0.018	92.54 \pm 0.009	97.61 \pm 0.015	85.73 \pm 0.017	66.98 \pm 0.011	87.48	32
	FedMask	85.32 \pm 0.033	61.38 \pm 0.057	68.71 \pm 0.046	81.32 \pm 0.024	84.32 \pm 0.044	92.01 \pm 0.025	62.28 \pm 0.037	57.12 \pm 0.029	74.06	1.0
	EDEN	87.11 \pm 0.006	65.89 \pm 0.009	79.16 \pm 0.008	86.36 \pm 0.006	85.21 \pm 0.012	91.24 \pm 0.010	69.59 \pm 0.012	62.07 \pm 0.011	78.33	0.703
	DeepReduce	86.71 \pm 0.071	64.98 \pm 0.091	60.32 \pm 0.061	84.42 \pm 0.044	84.09 \pm 0.057	92.37 \pm 0.041	64.91 \pm 0.043	55.72 \pm 0.078	73.61	1.123
	FedPM	90.31 \pm 0.016	74.66 \pm 0.019	87.03 \pm 0.017	91.42 \pm 0.021	89.79 \pm 0.013	95.57 \pm 0.015	74.80 \pm 0.014	62.19 \pm 0.017	83.22	0.946
	DeltaMask	89.52 \pm 0.021	74.01 \pm 0.033	86.86 \pm 0.024	92.27 \pm 0.027	89.68 \pm 0.014	94.94 \pm 0.019	74.09 \pm 0.029	61.56 \pm 0.030	82.87	0.197
$\rho = 1.0$	Linear Probing	93.97 \pm 0.004	74.11 \pm 0.009	59.26 \pm 0.011	89.40 \pm 0.008	89.47 \pm 0.005	95.35 \pm 0.003	76.64 \pm 0.009	61.72 \pm 0.012	79.99	-
	Fine-tuning	94.50 \pm 0.010	77.35 \pm 0.009	92.72 \pm 0.012	94.89 \pm 0.010	92.98 \pm 0.013	98.24 \pm 0.011	86.72 \pm 0.009	67.23 \pm 0.014	88.08	32
	FedMask	90.84 \pm 0.028	70.64 \pm 0.057	74.32 \pm 0.039	84.22 \pm 0.031	88.64 \pm 0.029	95.09 \pm 0.038	68.46 \pm 0.034	61.59 \pm 0.039	79.23	1.0
	EDEN	93.15 \pm 0.009	72.02 \pm 0.010	86.67 \pm 0.007	91.55 \pm 0.009	90.40 \pm 0.012	95.34 \pm 0.010	80.02 \pm 0.004	63.98 \pm 0.008	84.14	0.691
	DeepReduce	88.17 \pm 0.034	68.59 \pm 0.069	62.34 \pm 0.056	86.92 \pm 0.073	85.44 \pm 0.031	94.12 \pm 0.043	67.92 \pm 0.075	58.42 \pm 0.041	76.53	1.089
	FedPM	93.58 \pm 0.014	75.56 \pm 0.011	88.76 \pm 0.013	93.45 \pm 0.015	92.10 \pm 0.009	96.45 \pm 0.019	83.45 \pm 0.013	65.23 \pm 0.014	86.07	0.872
	DeltaMask	93.50 \pm 0.019	74.82 \pm 0.023	87.95 \pm 0.021	92.52 \pm 0.019	91.27 \pm 0.023	95.64 \pm 0.017	82.73 \pm 0.024	64.94 \pm 0.026	85.44	0.151

In Table 2, we note that DeltaMask achieves significant reductions in bitrate, while maintaining performance on par with Fine-tuning. This is particularly evident in scenarios with ρ less than 1, where DeltaMask ability to reduce bitrate without compromising on accuracy highlights its effectiveness in federated learning environments with varying levels of client participation.

C.3 Additional Experiments in non-IID settings

In this section, we provide additional experiments performed under non-IID settings, where we varied the participation rate (ρ). Similar to C.2, we include both Linear Probing and Fine-tuning for a rigorous evaluation. We report our findings in Table 3, where we also report the average bpp and accuracy across all tasks for a concise comparison of our baselines.

Table 3 reveals a notable improvement in DeltaMask performance, especially when the participation ratio

Table 3: Performance evaluation of DeltaMask (**Ours**) in terms of average bitrate (bits-per-parameter) during FL training using $Dir(0.1)$ over classes ($C_p \approx 0.2$ / **non-IID settings**) for CLIP ViT-B/32. Federated parameters are set to $N=30$ and $E=1$. For $\rho < 1$, clients are randomly selected.

	Method	CIFAR-10	CIFAR-100	SVHN	EMNIST	Fashion-MNIST	EuroSAT	Food-101	Cars196	Avg. Acc	Avg. bpp
$\rho = 0.2$	Linear Probing	84.51 \pm 0.019	49.04 \pm 0.022	43.16 \pm 0.020	82.41 \pm 0.035	86.29 \pm 0.024	91.63 \pm 0.022	51.54 \pm 0.021	47.92 \pm 0.038	67.06	-
	Fine-tuning	92.59 \pm 0.024	70.20 \pm 0.037	87.39 \pm 0.036	92.00 \pm 0.057	88.25 \pm 0.039	95.56 \pm 0.029	79.38 \pm 0.034	60.11 \pm 0.051	83.19	32
	FedMask	83.14 \pm 0.059	51.66 \pm 0.119	51.78 \pm 0.049	83.75 \pm 0.078	85.91 \pm 0.073	90.05 \pm 0.074	53.19 \pm 0.063	51.37 \pm 0.105	68.86	1.0
	EDEN	87.87 \pm 0.037	64.62 \pm 0.106	81.06 \pm 0.081	86.73 \pm 0.050	86.75 \pm 0.055	90.22 \pm 0.062	72.55 \pm 0.056	58.71 \pm 0.034	78.56	0.715
	DeepReduce	86.07 \pm 0.097	64.39 \pm 0.088	82.92 \pm 0.071	85.14 \pm 0.084	83.91 \pm 0.067	86.12 \pm 0.117	52.92 \pm 0.055	49.72 \pm 0.110	73.90	1.173
	FedPM	90.70 \pm 0.045	67.42 \pm 0.095	87.51 \pm 0.079	89.77 \pm 0.095	88.42 \pm 0.092	93.57 \pm 0.067	76.80 \pm 0.076	59.06 \pm 0.098	81.64	0.948
	DeltaMask	90.32 \pm 0.083	66.90 \pm 0.051	87.36 \pm 0.093	89.09 \pm 0.047	86.91 \pm 0.067	93.54 \pm 0.101	76.39 \pm 0.086	58.52 \pm 0.102	81.13	0.233
$\rho = 1.0$	Linear Probing	91.46 \pm 0.026	71.96 \pm 0.025	46.03 \pm 0.017	84.57 \pm 0.031	87.13 \pm 0.018	92.98 \pm 0.016	68.70 \pm 0.028	54.03 \pm 0.032	74.61	-
	Fine-tuning	93.61 \pm 0.048	75.49 \pm 0.052	90.10 \pm 0.063	93.13 \pm 0.037	91.06 \pm 0.041	97.02 \pm 0.034	84.71 \pm 0.013	64.93 \pm 0.063	86.26	32
	FedMask	88.42 \pm 0.051	63.04 \pm 0.081	64.32 \pm 0.073	86.41 \pm 0.039	86.39 \pm 0.044	91.67 \pm 0.031	68.04 \pm 0.050	54.39 \pm 0.089	75.34	1.0
	EDEN	92.14 \pm 0.043	71.65 \pm 0.060	86.28 \pm 0.057	90.87 \pm 0.046	89.94 \pm 0.034	93.26 \pm 0.035	78.79 \pm 0.083	61.18 \pm 0.027	83.01	0.703
	DeepReduce	87.33 \pm 0.052	67.19 \pm 0.061	83.19 \pm 0.048	85.71 \pm 0.082	84.52 \pm 0.075	92.12 \pm 0.060	69.11 \pm 0.092	60.31 \pm 0.094	78.69	1.092
	FedPM	92.99 \pm 0.045	74.34 \pm 0.023	89.35 \pm 0.025	92.65 \pm 0.098	91.33 \pm 0.041	95.37 \pm 0.048	83.69 \pm 0.076	63.65 \pm 0.074	85.42	0.901
	DeltaMask	92.84 \pm 0.083	73.69 \pm 0.051	89.01 \pm 0.085	91.92 \pm 0.089	91.27 \pm 0.055	94.54 \pm 0.103	83.48 \pm 0.081	63.47 \pm 0.096	85.03	0.191

ρ is less than 1, with only a 2% accuracy difference compared to Fine-tuning. This is a critical observation, since non-IID data distributions coupled with partial client participation closely mirror the conditions of real-world federated settings. Furthermore, our analysis shows that methods using stochastic mask training, such as DeepReduce and FedPM, yield better final model accuracy under non-IID conditions than traditional compression schemes like EDEN or hard-thresholding masking techniques like FedMask. Interestingly, the CLIP ViT-B/32 model excels in non-IID scenarios, underscoring the robust generalization abilities of pre-trained foundation models, which are particularly advantageous in non-IID federated environments. This emphasizes the importance of adapting these models for edge computing, capitalizing on their capability to effectively handle diverse and complex data distributions.

C.4 DeltaMask Efficiency on Edge Devices

In this section, we evaluate the runtime resource demands—computation and energy—of our probabilistic filter compression on three popular embedded platforms: NVIDIA Jetson Nano (4GB), Raspberry Pi 4 (4GB), and Coral Dev Board (1GB). These platforms were selected for their widespread use and capability to run machine learning tasks at the edge. To measure energy consumption, we used a Raspberry Pi 4 equipped with a Current/Power Monitor HAT, monitoring each device’s energy use with a 0.1 Ohm sampling resistor. Our tests, conducted over 5 runs, record the average runtime (in milliseconds) and energy usage (in nano Joules) for different probabilistic filters with varying bits per entry (8, 16, and 32), as detailed in Table 4.

Table 4: Average energy and latency benchmarking of the considered probabilistic filters across different devices. The CPU execution time (ms) and estimated energy consumption (nJ) per entry is computed over 10M entries.

Filter	Metric	Raspberry Pi 4	Coral Dev Board	Jetson Nano
Xor8	CPU Execution Time (ms)	0.942 \pm 0.0165	1.682 \pm 0.0059	0.479 \pm 0.0001
	Energy Consumption (nJ)	3.223 \pm 0.0023	2.826 \pm 0.0011	2.334 \pm 0.0012
Xor16	CPU Execution Time (ms)	0.955 \pm 0.0250	1.683 \pm 0.0008	0.502 \pm 0.0001
	Energy Consumption (nJ)	4.052 \pm 0.0032	3.580 \pm 0.0003	3.386 \pm 0.0016
Xor32	CPU Execution Time (ms)	0.978 \pm 0.0278	1.701 \pm 0.0006	0.539 \pm 0.0005
	Energy Consumption (nJ)	6.292 \pm 0.0021	4.732 \pm 0.0008	4.692 \pm 0.0023
BFuse8	CPU Execution Time (ms)	0.587 \pm 0.0059	1.144 \pm 0.0035	0.289 \pm 0.0013
	Energy Consumption (nJ)	2.045 \pm 0.0019	1.979 \pm 0.0015	1.829 \pm 0.0023
BFuse16	CPU Execution Time (ms)	0.590 \pm 0.0066	1.183 \pm 0.0029	0.282 \pm 0.0002
	Energy Consumption (nJ)	3.262 \pm 0.0020	2.898 \pm 0.0017	2.157 \pm 0.0033
BFuse32	CPU Execution Time (ms)	0.612 \pm 0.0054	1.201 \pm 0.0017	0.301 \pm 0.0002
	Energy Consumption (nJ)	4.021 \pm 0.0026	3.771 \pm 0.0022	3.263 \pm 0.0012

Table 5: Evaluating Classifier Initialization Schemes in `DeltaMask`. Comparing Average Bitrate and Accuracy in FL Training using $Dir(10)$ over classes ($C_p \approx 1.0$ / **IID settings**) for CLIP ViT-B/32. Federated parameters are set to $N=30$ and $E=1$.

Method	CIFAR-10	CIFAR-100	SVHN	EMNIST	Fashion-MNIST	EuroSAT	Food-101	Cars196	Avg. Acc	Avg. bpp
Fine-tuning	94.50 \pm 0.010	77.35 \pm 0.009	92.72 \pm 0.012	94.89 \pm 0.010	92.98 \pm 0.013	98.24 \pm 0.011	86.72 \pm 0.009	67.23 \pm 0.014	88.08	32
<code>DeltaMask_{He}</code>	90.28 \pm 0.052	67.34 \pm 0.069	84.09 \pm 0.063	87.32 \pm 0.081	87.69 \pm 0.034	93.22 \pm 0.073	78.05 \pm 0.028	58.74 \pm 0.084	80.84	0.143
<code>DeltaMask_{FiT}</code>	93.42 \pm 0.023	71.17 \pm 0.041	86.31 \pm 0.039	92.09 \pm 0.021	89.87 \pm 0.026	95.53 \pm 0.019	81.71 \pm 0.033	60.01 \pm 0.029	83.76	0.145
<code>DeltaMask_{LP}</code>	93.50 \pm 0.019	74.82 \pm 0.023	87.95 \pm 0.021	92.52 \pm 0.019	91.27 \pm 0.023	95.64 \pm 0.017	82.73 \pm 0.024	64.94 \pm 0.026	85.44	0.151

From the results, we clearly notice that all filter variants demand limited computational resources, both in terms of execution time and energy requirements. `BFuse8` is particularly notable for its efficiency, requiring only an average execution time of 0.673 milliseconds and consuming just 1.95 nano Joules of energy across the considered devices. This underscores the practicality of our probabilistic filter-based compression scheme in federated settings, where devices are often constrained by limited computational capabilities and strict energy budgets. Additionally, our analysis shows that even with an increase in the bits-per-entry (bpe) parameter, the rise in execution time and energy consumption is quite modest. This is particularly noteworthy given the simultaneous improvement in the false positive rate, which is inversely proportional to 2^{-bpe} . This pattern suggests a beneficial trade-off between accuracy and resource utilization, reinforcing the adaptability and effectiveness of our approach in federated learning scenarios that prioritize computational efficiency and energy conservation.

C.5 Comparing Classifier Heads in `DeltaMask`

In `DeltaMask`, we enable the classification head to adapt in a single linear probing round, while freezing the rest of the model. This approach produces more stable outcomes and quicker convergence than previous methods [Isik et al. \(2023b\)](#); [Zhou et al. \(2020\)](#); [Ramanujan et al. \(2020\)](#); [Zhou et al. \(2020\)](#) that used Kaiming initialization to identify high-performing subnetworks in randomly initialized networks. Although the classification head typically has fewer parameters, scenarios requiring extremely low bitrates make transmitting even a single round’s floating-point weights impractical. In this section, we explore such situations, investigating different alternatives for the classifier layer. Specifically, we replace the linear classifier with a Gaussian Naive Bayes classifier from `FiT` [Shysheya et al. \(2022\)](#), specifically `FIT-LDA`. This classifier is data-driven, with a minimal number of learnable parameters (2 float-point values), making it ideal for our purpose. In our analysis, we utilize CLIP ViT-B/32, masking the last five transformer blocks and compare `DeltaMaskFiT` against both a single-round trained linear classifier (`DeltaMaskLP`) and a Kaiming initialized (frozen) classifier (`DeltaMaskHe`).

From Table 5, we notice that `DeltaMaskLP` outperforms other initialization methods by over 2% without significantly increasing the bitrate, while `FiT` can be an effective alternative to Kaiming initialization, increasing accuracy by $\approx 3\%$. More importantly, these findings highlight the importance of appropriate classifier layer initialization during fine-tuning of foundation models in downstream tasks. However, we demonstrate that a single fine-tuning round of the classifier layer, with the remaining model frozen, is an effective strategy with minimal impact on the communicated bitrate.